Performance of rotor-only axial fans designed for minimum exit kinetic energy

S.J. van der Spuy[1] T.W. von Backström[1]

(First received April 2002; Final version July 2002)

The major loss source in rotor-only axial fans is the kinetic energy associated with the axial and circumferential components of the exit flow. This paper investigated the aerodynamic and acoustic performance of two fans designed to produce minimum exit kinetic energy. The first was a general application fan and the second a low-noise fan with large-chord forward-swept blades. The fans were tested for fan noise and performance in accordance with BS 848. The low-noise fan was the quieter and more efficient of the two fans, whilst both fans were quieter and more efficient than an existing typical general application fan, of unknown design. The results underlined the importance of following a well-defined design methodology when designing rotor-only axial flow fans.

Nomenclature

a	outer-to-inner radius ratio
A	dimensionless work rate
B	dimensionless flow rate
c	chord length, m
C	absolute velocity, m/s
C_w	absolute swirl velocity, m/s
C_a	absolute axial velocity, m/s
L	kinetic energy flux, W
i	incidence angle, °
m	deviation angle coefficient
M_R	radial Mach number
s	blade pitch, m
r	fan radius, m
u	dimensionless swirl velocity $= C_w/(r_i\Omega)$
U	blade speed, m/s
v	dimensionless axial velocity $= C_a/(r_i\Omega)$

Greek

α	angle of attack, °
β	relative flow angle, °
γ	pitch angle (from circumferential), °
δ	deviation angle, °
Δ	change in value
ϕ	flow coefficient, C_a/U_o
η	geometric blade sweep angle, °
η	efficiency
λ	aerodynamic blade sweep angle, °
ν	hub-tip ratio
ρ	density, kg/m^3
θ	camber angle, °
θ_s	blade axis sweep angle, °
σ	solidity = c/s
ψ	load coefficient, $\Delta p/\left(\frac{1}{2}\rho U_o{}^2\right)$
ξ	stagger angle (from axial), °
Ω	rotational speed, rad/s

Subscripts

a	axial
i	inner radius
m	mean value
o	outer radius
s	"swept" blade variables
w	whirl
1	blade leading edge
2	blade trailing edge
$infinite$	axial distance far up- or downstream from rotor

1. Department of Mechanical Engineering, University of Stellenbosch, Private Bag X1, Matieland, 7602 South Africa

Introduction

In rotor-only axial fans designed according to simple traditional rules, the kinetic energy associated with the axial and circumferential components of the exit flow can be almost as large as the useful fan work.[1] The stagnation pressure losses associated with the blade profile, wall friction at the casing and hub, or tip clearance are much smaller than those associated with the exit kinetic energy. The latter have a major effect on the fan efficiency because the exit dynamic pressure in axial fans is large compared to the fan pressure rise, and rotor-only fans never have stator blade rows and rarely have diffusers to increase exit static pressure.

The theory required for the minimisation of exit kinetic energy for a rotor-only axial fan is described by Von Backström *et al.*[1] The main objective of the work presented here was to motivate the use of a well-defined design methodology when designing axial fans, by reporting on the measured aerodynamic and acoustic performance of two rotor-only fans designed for minimal kinetic energy in the flow leaving the rotor. The one fan is a member of a typical general application series of fans (Fig. 1), while the other is a one-off design aimed at low noise generation (Fig. 2). The term "fan series" refers to a scenario where one blade design is used for a number of different fan outer diameter sizes by cutting (also referred to as cropping) the blade to the desired length. The term "general application" refers

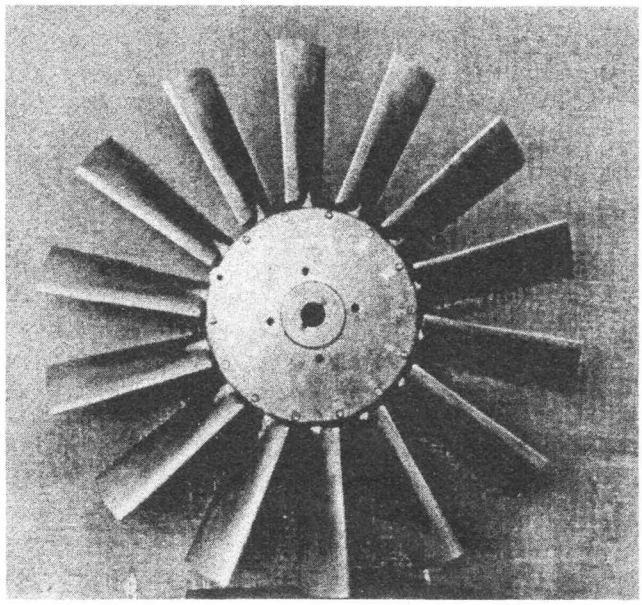

Fig. 1. Photograph of 14-bladed, 630 mm diameter, general application fan

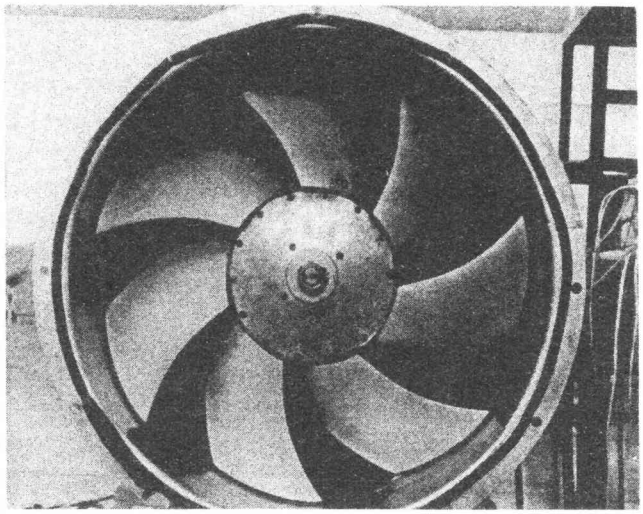

Fig. 2. Photograph of 7-bladed, 630 mm diameter, low-noise fan

to fans typically used in the air-conditioning and building ventilation industry. The performance of the general application and low-noise fan is compared with that of an industry-related "reference fan" with the same "fan series" range as that of the general application fan (the design specifications of the reference fan are not known).

According to Wright,[2], Wright & Simmons,[3] and Van der Spek,[4] the following variables affect axial fan noise most strongly: blade tip speed, blade aspect ratio and blade forward sweep angle. Mesquita *et al.*[5] proposed an axial flow design method where the blade airfoil profile at hub and shroud is optimised for minimum drag and the profile distribution is based on a free vortex outlet velocity profile. Bruneau[6] used elementary airfoil theory, combined with a generic power law equation for the exit velocity profile, to design axial fan blades, whilst Beiler & Carolus[7] used the same theory, combined with corrections for sweep angles, to design forward-swept axial fan blades. References to the effect of minimisation of the exit kinetic energy on fan aerodynamic or acoustic performance were not found in the literature, despite a wide search.

Van der Spuy[8] designed two fan types to investigate how the minimisation of fan exit kinetic energy affects fan total-to-static efficiency and fan noise. The first was a general application fan series, ranging from 315 mm to 1 000 mm diameter (Fig. 1), and the second a 630 mm diameter low-noise fan with large-chord forward-swept blades (Fig. 2).

Optimisation procedure

Von Backstrom *et al.*[1] determined optimum exit velocity profiles for rotor-only fans by minimising the functional representing exit kinetic energy, for given flow and load coefficients:

$$L = \pi \times \rho \times \int_{r_i}^{r_o} r C_a \left({C_a}^2 + {C_w}^2 \right) dr \tag{1}$$

The constraints according to which the functional was minimised are:

Radial equilibrium:

$$\Omega \times \left[\frac{d\left(C_w r\right)}{dr} \right] = \frac{C_w}{r} \times \left[\frac{d\left(C_w r\right)}{dr} \right] + C_a \times \frac{dC_a}{dr} \tag{2}$$

Prescribed dimensionless work rate:

$$A = \frac{1}{\Omega^2 \times {r_i}^5} \int_{r_i}^{r_o} r^2 C_a C_w dr \tag{3}$$

Prescribed dimensionless flow rate:

$$B = \frac{1}{\Omega^2 \times {r_i}^3} \int_{r_i}^{r_o} r \; C_a dr \tag{4}$$

The minimisation problem was discretised for solution as a numerical problem for values of A and B and tip-to-hub diameter ratio, a, and solved by sequential quadratic programming.[1] The values for A and B were based on given load and flow coefficients. This approach resulted in exit velocity profiles requiring blades with less twist than the more traditional free vortex velocity distribution. Fig. 3 compares typical exit axial and swirl velocity components for a free vortex and an optimised radial swirl velocity distribution.

Design approach

The book by Wallis[9] on the design of axial flow fans was used for the design procedure. Articles by Wright & Simmons[3] and Smith & Hsuan[10] were used to adapt the design procedure for the forward swept fan blade of the low-noise fan. The design procedures used for both the general application and low noise fans are described by Van der Spuy.[8]

The designs were constrained by industry-related specifications for a general application fan series. This determined the casing diameters, hub diameters and hub-tip ratios, ν, as well as the number of blades. The 150 mm

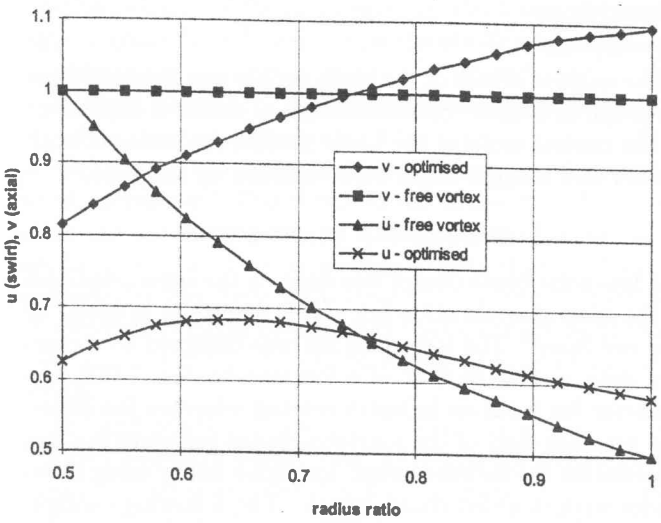

Fig. 3. Example of optimised and free vortex velocity profiles for $v = \phi = \psi = 0.5$ (Von Backström *et al.*[1])

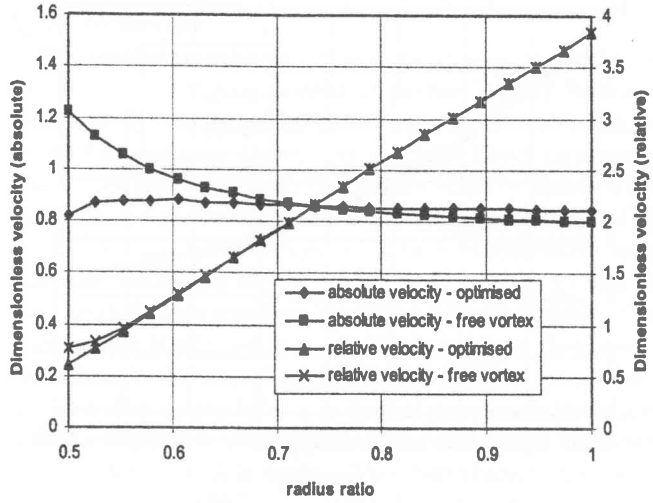

Fig. 4. Absolute and relative velocities for optimised and free vortex velocity profiles ($v = 0.25; \phi = 0.19; \psi = 0.12$)

diameter hubs could carry either five or ten blades and the 250 mm diameter hubs either seven (half solidity) or fourteen (full solidity). A complete series of general application fans was designed, ranging from 315 mm to 1 000 mm diameter in eight steps for standard duct sizes. The smaller diameter fans required cropping of the standard blade. Only one size low-noise fan, 630 mm in diameter, was built, since the forward swept blade was not suitable for cropping.

Flow and work rate values in equations (3) and (4) were chosen based on flow and load coefficients that are competitive with an existing fan series. They were applied to the range of different fan sizes for a few selected hub diameters with full or half sets of blades.

General application fan design

The velocity profiles obtained from the procedure for minimising the exit kinetic energy served as basis for calculating the relative inlet and exit flow angles. The axial inlet velocity profile used in the design was uniform with zero whirl. From the relative inlet and exit flow angles the flow deflection and mean flow angle in the rotor were calculated and used as approximate indications of blade camber and blade twist to compare the different configurations. From these we chose a representative combination as design specification for the whole series: $\nu = 0.25, \phi = 0.19, \psi = 0.12$. This combination refers to a 1 000 mm diameter fan with a 250 mm hub and half solidity (seven blades) and represented the best average radial distribution of blade camber and stagger. Basing the design on the largest specified fan diameter and longest possible blade also eliminated the need for extrapolation of the blade shape.

The exit kinetic energy for the optimised velocity distribution of the general application fan was calculated as 37.7 % of the fan effective power, compared to a value of 38.6 % for a free vortex velocity distribution, based on the same constraints and design parameters, i.e. a reduction of 2.3% of the exit kinetic energy. The effect of the optimised velocity profile is illustrated more clearly in Fig. 4, where the absolute and relative profiles of dimensionless velocity for the free vortex and optimised distributions, for $\nu = 0.25, \phi = 0.19, \psi = 0.12$, are shown. The velocity values are normalised by dividing with the circumferential velocity of the fan blade at the hub. The optimised absolute velocity values vary less between rotor hub and tip than those of the free vortex velocity values (0.05 compared to 0.4). The absolute velocity profile for the optimised distribution shows an almost constant trend between rotor hub and tip, as opposed to the decreasing trend of the free vortex distribution. The dimensionless value for optimised absolute velocity at the hub is considerably less than the value for free vortex absolute velocity at the hub (0.81 compared to 1.21). The small flow coefficient value, $\phi = 0.19$, means that the relative velocity distributions are dominated by the circumferential velocity of the fan (as shown by the near linear trend). The large difference in absolute velocity distribution at the hub is also evident in the higher relative free vortex velocity values, when compared to the optimised profile.

To allow for streamline curvature, "actuator disk theory" was applied to the calculated velocity distribution to determine the velocity profiles at the leading and trailing edge of the fan blade[11] (Figs. 5 and 6). Because of its high lift-drag ratio the fan blade design was based on the F-series profile of Wallis.[9,12]

Chord lengths and lift coefficients

Using the velocity distribution obtained, the blade loading factor, $C_L\sigma$, was calculated:

$$C_L\sigma = 2 \times \left(\frac{C_{w2}}{C_{am}}\right) \times \cos\beta_m \qquad (5)$$

The chord lengths at the hub and tip were calculated

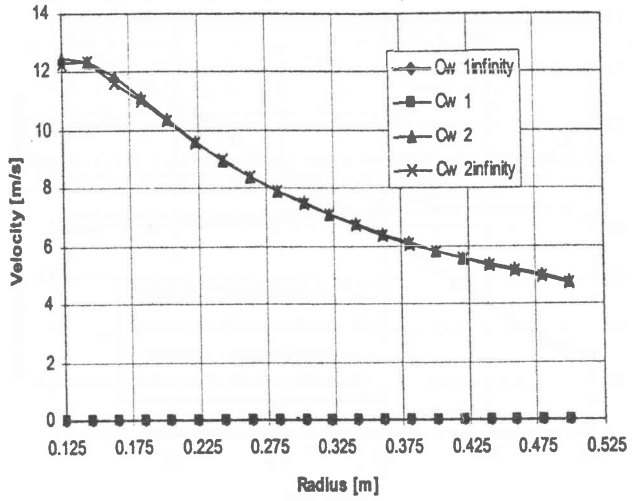

Fig. 5. Swirl velocity profiles for general application fan design

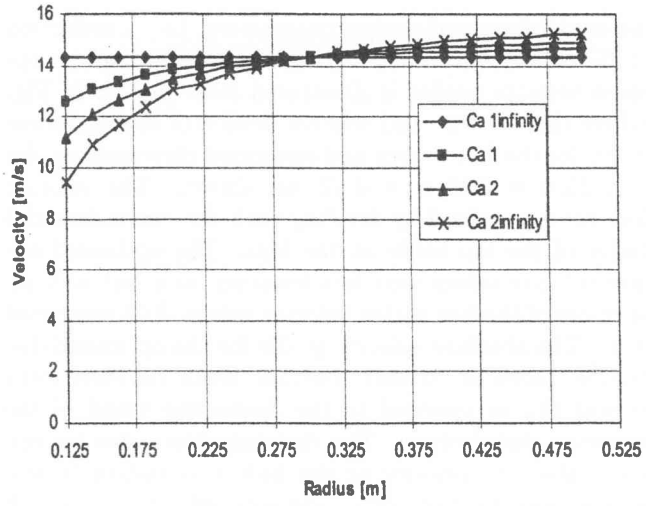

Fig. 6. Axial velocity profiles for general application fan design

by choosing appropriate values for C_L at the hub and tip and inserting them into equation (5). Linear interpolation between hub and tip gave the intermediate chord lengths and allowed calculation of the lift coefficient distribution along the blade length. The hub and tip chord lengths of the uncropped general application fan blade were 87 and 71 mm.

Blade camber and stagger

The values for camber angle were obtained using:

$$\theta = \beta_1 - \beta_2 + \delta - i \tag{6}$$

The values for incidence angle were taken from a graph in Wallis,[9] whilst the values for δ were calculated using an equation from Carter:[13]

$$\delta = \left(m \times (\beta_1 - \beta_2) \times \sqrt{\frac{s}{c}}\right) / \left(1 - m \times \sqrt{\frac{s}{c}}\right) \tag{7}$$

The value for m was calculated as a function of stagger angle, using a curve fit of Bruneau.[6] The stagger angle followed from:

$$\xi = \beta_1 - \alpha \tag{8}$$

The angle of attack of the blade profile was obtained from the graph in Wallis.[9] Since the angle of attack is dependent on the camber angle of the blade profile, the values of both camber and stagger angle were obtained by iteration.

Low-noise fan blade design

The low-noise blade design was done on the same principles as the general application fan and is described in detail by Van der Spuy.[8] The low-noise fan was designed to a pressure duty similar to that of a fourteen-bladed, 1 000 mm diameter fan from an industry-related reference fan series. The pressure duty of the fourteen-bladed reference fan was achieved for the forward swept, low-noise fan by using seven blades with doubled chord length. The following configuration was used in the design process: $\nu = 0.25$, $\phi = 0.2$, $\psi = 0.21$.

The exit velocity profiles were calculated in the same way as for the general application fan. F-series airfoils were also used for the low-noise fan.

Low noise fan blade sweep

The low-noise fan design allowed blade forward sweep. Wright & Simmons[3] provided a set of sweep-angle curves for various wave number modes from which a single suitable curve was selected.

$$\eta = 37.9261 + 79.1634 \times M_R - 0.3152/M_R - 23.0131 \times M_R^3 \tag{9}$$

where η represents the blade sweep angle viewed perpendicularly from the upstream side of the axial flow fan, in the plane perpendicular to the fan shaft and M_R is the radial Mach number based on fan rotational speed. M_R gives an indication of the degree of misalignment between the disturbance and the direction of motion of the blade, i.e. a higher misalignment requires a higher sweep angle.[3] Referring to Smith & Hsuan[10] and Beiler & Carolus[7] the aerodynamic sweep angle, λ was defined. It represents the sweep when viewed perpendicular to the plane connecting the blade sectional chord lines. The complimentary blade stagger angle, $\gamma = 90 - \xi$ was used here:

$$\tan \lambda = \tan \eta \times \cos \gamma \tag{10}$$

All the blade variables were transformed by the angle λ at the different radii.

The preliminary stagger angle was assumed to be equal to β_m, in order to calculate the value for geometric sweep at different radial locations. Once the aerodynamic sweep was calculated, the "swept" values for the flow angles were calculated:

$$\beta_s = \tan^{-1}(\tan \beta \times \cos \lambda) \tag{11}$$

These were used to calculate the blade loading factor and the values for solidity ratio, σ, at the fan hub and tip were calculated by selecting lift coefficient values at the hub and tip. Once the values for solidity ratio at the blade hub and tip were calculated, the values for "swept" blade spacing and chord at the hub and tip were calculated:[10]

$$s_s = s/\sqrt{1+(\tan\eta)^2} \quad (12)$$

$$c_s = \sigma \times s_s \quad (13)$$

Interpolating linearly between the "swept" chord values at the hub and tip gave the "swept" chord and solidity distribution over the blade length.

The values for the solidity distribution were used to calculate the lift coefficient distribution along the blade length. The "swept" camber angle distribution was then calculated:

$$\theta_s = \beta_{s1} - \beta_{s2} + \delta - i \quad (14)$$

where δ and i were determined as before.

The "swept" stagger angle distribution followed:

$$\xi_s = \beta_{s1} - \alpha \quad (15)$$

Finally, the "unswept" values for stagger and camber angle at the different radii were calculated:

$$\xi = \tan^{-1}(\tan\xi_s/\cos\lambda) \quad (16)$$

$$\theta = \tan^{-1}(\tan\theta_s/\cos\lambda) \quad (17)$$

Fan test equipment

A selection of fan sizes was tested on a BS 848, type D, fan test facility at various blade setting angles. The Standards[14,15] were adjusted to provide a test facility on which noise and performance tests could be executed simultaneously, by removing the downstream flow straightener.[8] The 630 mm diameter general application fan was set at a blade angle for the same pressure characteristic as the 630 mm diameter low-noise fan to enable a comparison between the two fans, using the fan scaling laws. The low-noise fan was tested at a constant blade setting angle.

Results

The values of total efficiency, static pressure and sound power level were determined as prescribed by the Standards.[14,15] The curves for the design specification general application fan surround the design point well (Fig. 7) for the blade setting angles originally specified to give an even distribution of the blade operating range on either side of the design point.

General application fan

The twist in the long blades of the large diameter fans caused negative blade tip incidence angles at large blade stagger settings (blade chords nearly in plane of rotation). This was counteracted by the open flow passages and large lift coefficients owing to a relatively larger effective angle of attack near the fan hub contributing more to the functioning of the blade at larger stagger settings (when compared to the reference fan). The blade twist also led to a relatively high angle of attack at the hub for large blade setting angles, implying that stall could occur readily for the large blade setting angles once the system resistance started increasing (Fig. 8).

The general application fan showed higher efficiency values (7% to 10% increase) than that of the reference fan series (the design specifications of the reference fan series were not known), which can be attributed to the optimisation of the design as described (Fig. 9).

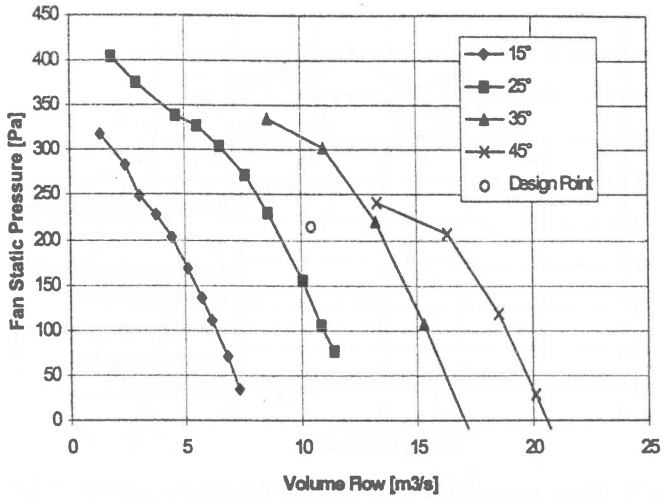

Fig. 7. Test data for 1000/250/7/720 fan, scaled to 1440 r.p.m. and compared with design point

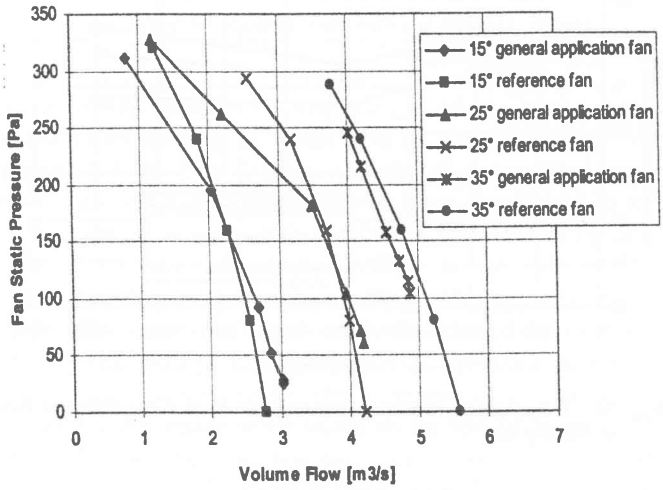

Fig. 8. Comparison of fan static pressure for general application fan and reference fan for 630/150/10/1440 configuration

Low-noise fan

The small number of blades, combined with the large chords used for the low-noise fan, prevented the closing of the air passage surrounding the hub. The forward sweep meant that the proper tip clearance with no interference with the casing was possible at only one blade stagger setting.

As mentioned before, the low comparative noise level of both the low noise and the general application fan could partially be ascribed to the use of the optimised velocity profiles in the design procedures, because fan noise can be related to a loss of energy in a fan (Fig. 10).

Although the low-noise fan was tested at 1 200 r.p.m., its aerodynamic performance was geometrically scaled to 1 440 r.p.m. to enable a direct comparison with the general application fan (Figs. 11 and 12). The figures also

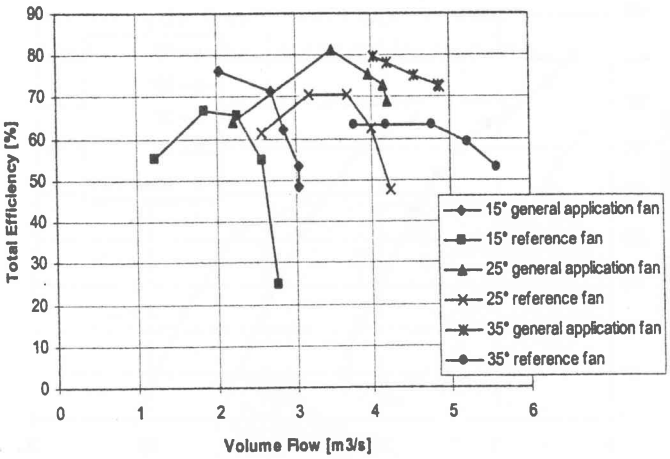

Fig. 9. Comparison of fan total efficiency for general application fan and reference fan for 630/150/10/1440 configuration

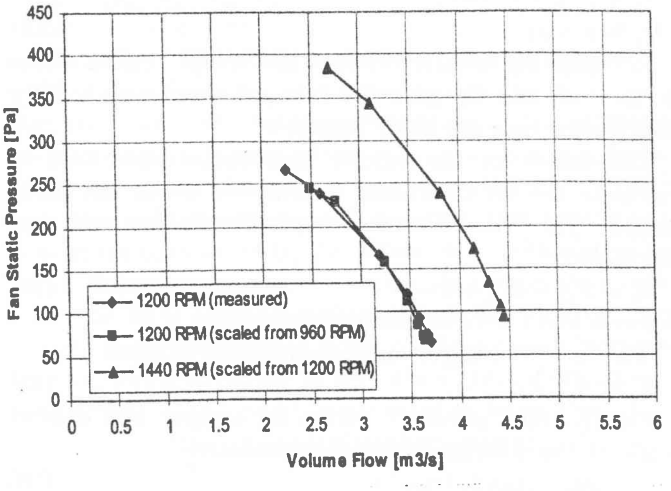

Fig. 11. Static pressure measured and scaled for low-noise fan at 1200 r.p.m. and 1440 r.p.m.

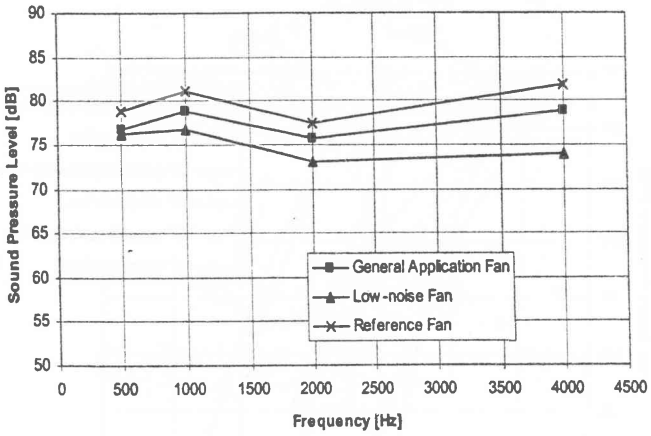

Fig. 10. Comparison of sound pressure levels of three different fans at 960 r.p.m.

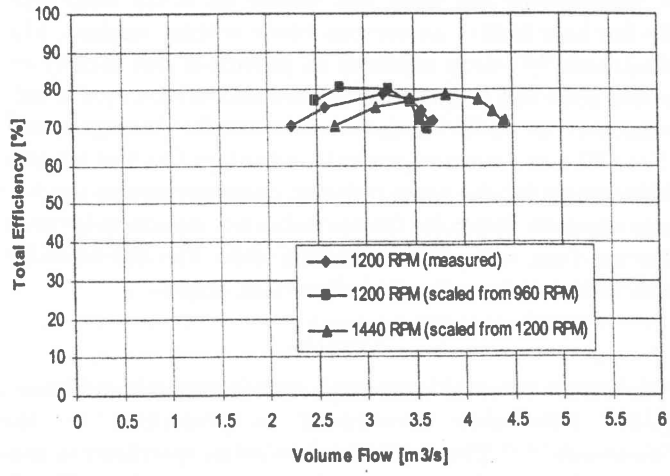

Fig. 12. Total efficiency measured and scaled for low-noise fan at 1200 r.p.m. and 1440 r.p.m.

show measured results at 1 200 r.p.m. compared to values scaled from 960 r.p.m., to verify the reliability of the scaling. Based on a direct comparison of results at 1 440 r.p.m., the low noise fan has a larger static pressure rise than the other two fans tested, although the 70% to 80% efficiency values of the general application fan and the low-noise fan are within the same size-range (Figs. 9 and 12). The higher pressure rise of the low-noise fan can be attributed to its higher solidity (equivalent to 14 short chord blades, not 10).

Conclusions

The low-noise fan had a high fan total efficiency, high static pressure rise, and a low noise level (Table I). The designed general application fan was as efficient and marginally noisier (looking at frequencies between 500 Hz and 4 000 Hz in Fig. 10) than the low-noise fan, due to the smaller chord length and unswept blade plan form (Table I). The designed general application fan was however considerably quieter and more efficient than the reference fan (Table I). This improvement could be attributed to the use of the minimised exit kinetic energy velocity profile, since the blade tip speed, blade chord length, number of blades, and unswept blade plan form for both the reference and general application fans were similar.

The designed general application fan was a good compromise, since it was as cheap to manufacture as the reference fan, but its efficiency was comparable to that of the low-noise fan, and its noise values were roughly half-way between those of the reference fan and the low-noise fan. The main contributor to axial rotor-only fan noise is blade tip speed. If electric motor speed control capability is available, the low-noise fan speed may be reduced to a level that gives the same pressure rise values as for the general application fan, at considerably lower noise emission levels. The manufacturing of a low-noise fan, combined with electric motor speed control would however be costly. Based on the above results, when comparing axial fans running at

the same rotational speed, design methodology is the main contributor towards improving fan efficiency and noise levels.

TABLE I
SUMMARY OF RESULTS

	Maximum total efficiency [%]	Maximum static pressure [Pa]	Sound pressure level @ 400 Hz [dB]
Reference fan	70	295	82
General application fan	80	325	79
Low-noise fan	78	380	74

REFERENCES

[1] Von Backström TW, Buys JD & Stinnes WH. Minimisation of the Exit Loss of a Rotor-only Axial Fan. *Engineering Optimization*, 1996, **26**, pp.28–29.

[2] Wright SE. The Acoustic Spectrum of Axial Flow Machines. *Journal of Sound and Vibration*, Part 2, 1976, **45**, p.193.

[3] Wright T & Simmons WE. Blade Sweep for Low-Speed Axial Fans. *ASME Paper GT-53*, 1989, pp.1–6.

[4] Van der Spek HF. Advanced Low Noise Cooling Fans. 9th *Cooling Tower and Spraying Pond Symposium IAHR*, Von Karman Institute for Fluid Dynamics, Brussels, 1994, pp.3–4.

[5] Mesquita ALA, Serra CMV, Cruz DOdA & Filho NM. A Simplified Method for Axial Flow Turbomachinery Design. *Journal of the Brazilian Society of Mechanical Sciences*, **XXI**, 1999, pp.61–70.

[6] Bruneau PRP. The Design of a Single Rotor Axial Flow Fan for a Cooling Tower Application. MEng thesis, University of Stellenbosch, 1994.

[7] Beiler MG & Carolus TH. Computation and Measurement of the Flow in Axial Flow fans with Skewed Blades. *ASME Journal of Turbo machinery*, 1999, **121**, pp.59–66.

[8] Van der Spuy SJ. The Design of a Low-noise Rotor-only Axial Flow Fan Series. MEng thesis, University of Stellenbosch, 1997.

[9] Wallis RA. *Axial Flow Fans and Ducts*. John Wiley & Sons, Inc. 1983, pp.147–170, 197–200.

[10] Smith LH & Yeh H. Sweep and Dihedral Effects in Axial Flow Turbomachinery. *Transactions of the ASME, Journal of Basic Engineering*, 1963, **85**, pp.401–405.

[11] Dixon SL. *Fluid Mechanics–Thermodynamics of Turbomachinery*. 3rd edn, William Clowes Ltd., Great Britain, 1978.

[12] Wallis RA. The Development of Blade Sections for Axial Flow Fans. *Instn. Engrs. Aus., Mechanical and Chemical Engineering Transactions*, 1972, p.116.

[13] Carter ADS. The Low Speed Performance of Related Aerosols in Cascades. *Gt. Britain Aer. Research Council ARC CP 29*,1950.

[14] British Standards Institution. Fans for General Purpose, Part 1, Methods of Testing Performance. *BS 848*, 1980.

[15] British Standards Institution. Fans for General Purpose, Part 2, Methods of Noise Testing. *BS 848*, 1985.